High-throughput identification of small molecules that affect human embryonic vascular development

Helena Vazão[a,1], Susana Rosa[a,1], Tânia Barata[a,b], Ricardo Costa[c], Patrícia R. Pitrez[a], Inês Honório[a], Margreet R. de Vries[d], Dimitri Papatsenko[e], Rui Benedito[c], Daniel Saris[b], Ali Khademhosseini[f,g,h,i,j], Paul H. A. Quax[d], Carlos F. Pereira[a], Nadia Mercader[k], Hugo Fernandes[a,b], and Lino Ferreira[a,l,2]

[a]Center for Neurosciences and Cell Biology, University of Coimbra, 3000 Coimbra, Portugal; [b]MIRA Institute for Biomedical Engineering and Technical Medicine, University Twente, Enschede, 7500AE, The Netherlands; [c]Department of Cardiovascular Development and Repair, Centro Nacional de Investigaciones Cardiovasculares Carlos III, 28029 Madrid, Spain; [d]Einthoven Laboratory for Experimental Vascular Medicine, Leiden University Medical Center, 2333 ZA Leiden, The Netherlands; [e]Black Family Stem Cell Institute, Icahn School of Medicine at Mount Sinai, New York, NY 10029; [f]Center for Biomedical Engineering, Department of Medicine, Brigham and Women's Hospital, Harvard Medical School, Boston, MA 02115; [g]Harvard-Massachusetts Institute of Technology Division of Health Sciences and Technology, Massachusetts Institute of Technology, Cambridge, MA 02139; [h]Wyss Institute for Biologically Inspired Engineering, Harvard University, Boston, MA 02115; [i]Department of Maxillofacial Biomedical Engineering and Institute of Oral Biology, School of Dentistry, Kyung Hee University, Seoul 130-701, Republic of Korea; [j]Department of Physics, King Abdulaziz University, Jeddah 21569, Saudi Arabia; [k]Institute of Anatomy, University of Bern, 3012 Bern, Switzerland; and [l]Faculty of Medicine, University of Coimbra, 3000 Coimbra, Portugal

Edited by Michael A. Gimbrone, Brigham and Women's Hospital, Boston, MA, and approved March 2, 2017 (received for review October 27, 2016)

Birth defects, which are in part caused by exposure to environmental chemicals and pharmaceutical drugs, affect 1 in every 33 babies born in the United States each year. The current standard to screen drugs that affect embryonic development is based on prenatal animal testing; however, this approach yields low-throughput and limited mechanistic information regarding the biological pathways and potential adverse consequences in humans. To develop a screening platform for molecules that affect human embryonic development based on endothelial cells (ECs) derived from human pluripotent stem cells, we differentiated human pluripotent stem cells into embryonic ECs and induced their maturation under arterial flow conditions. These cells were then used to screen compounds that specifically affect embryonic vasculature. Using this platform, we have identified two compounds that have higher inhibitory effect in embryonic than postnatal ECs. One of them was fluphenazine (an antipsychotic), which inhibits calmodulin kinase II. The other compound was pyrrolopyrimidine (an antiinflammatory agent), which inhibits vascular endothelial growth factor receptor 2 (VEGFR2), decreases EC viability, induces an inflammatory response, and disrupts preformed vascular networks. The vascular effect of the pyrrolopyrimidine was further validated in prenatal vs. adult mouse ECs and in embryonic and adult zebrafish. We developed a platform based on human pluripotent stem cell-derived ECs for drug screening, which may open new avenues of research for the study and modulation of embryonic vasculature.

high-throughput screening | endothelial cells | vascular toxicity | pluripotent stem cells | embryonic endothelial markers

The development of platforms for the rapid profiling of chemical/pharmaceutical substances that have an effect on embryonic development is of great interest to reduce human embryo lethality and birth defects (1). In the United States, ∼3% of all babies born each year have birth defects (https://www.cdc.gov/ncbddd/birthdefects/data.html). The majority of birth defects were the result of multiple environmental and/or genetic effects that acted in concert. Environmental causes included pesticides, pharmaceuticals, solvents, metals, and air pollutants (2). The cardiovascular system is the first functional organ to develop in the mammalian embryo, and thus, the disruption of the vascular system is important for the identification of compounds with developmental toxicity (3, 4). Disruption of vascular development has been correlated with fetal loss, human malformations, and cognitive impairment (5, 6). Standard protocols for assessing the effect of chemicals on vascular development involve testing on animals. Unfortunately, these tests are low-throughput, expensive, yield limited mechanistic information, and do not account for differences between species. Recent approaches combining high-throughput screening and high-content screening platforms with computational systems modeling have been used for the identification of vascular-disruptive developmental drugs (3, 4); however, they do not account for differences between species.

Human pluripotent stem cells (hPSCs) represent a potential source of embryonic endothelial cells (ECs) (7). hPSC-derived ECs have not been used for the identification of molecules that disrupt vascular development, in part because it is relatively unknown whether hPSC-derived ECs exhibit embryonic features, because a set of markers to distinguish embryonic ECs from postnatal ECs has to be identified. In addition, it requires the validation of the hits identified in static screening conditions under flow conditions to replicate the hemodynamics of blood vessels. Approaches to mimic the hemodynamic forces experienced by vessels in vivo require the development of microfluidic platforms. Recently, researchers have replicated the circular cross-section of blood vessels in microfluidic devices (8); however, these tools have not been used in the context of drug screening. Moreover, it requires a final validation of the hits in animal embryos.

Here, we report a platform suitable for the high-throughput screening of compounds that affect embryonic vascular development.

Significance

It is well recognized that several chemicals and/or drugs are potentially harmful if used during pregnancy. Unfortunately, systems capable of predicting which drugs affect embryonic development rely almost exclusively on prenatal animal testing, with all the associated limitations. Using human pluripotent stem cells, we developed a fully humanized system capable of predicting which drugs affect, specifically, vascular embryonic development. The system was used to screen a library of chemicals (1,280 drugs), and two compounds were identified as specific inhibitors of human embryonic vasculature. The platform described here is a valid alternative to animal testing and can be used to screen existing and newly developed drugs.

Author contributions: H.V., S.R., R.B., D.S., A.K., P.H.A.Q., H.F., and L.F. designed research; H.V., S.R., T.B., R.C., P.R.P., I.H., M.R.d.V., D.P., R.B., C.F.P., N.M., H.F., and L.F. performed research; H.V., S.R., T.B., R.C., P.R.P., I.H., M.R.d.V., D.P., R.B., D.S., A.K., P.H.A.Q., C.F.P., N.M., H.F., and L.F. analyzed data; and H.V., H.F., and L.F. wrote the paper.

Conflict of interest statement: A patent has been filed for this work ("Differentiated Cell Population of Endothelial Cells Derived from Human Pluripotent Stem Cells, Composition System, Kit and Uses Therefore"; PCT/IB2013/061110).

This article is a PNAS Direct Submission.

[1]H.V. and S.R. contributed equally to this work.

[2]To whom correspondence should be addressed. Email: lino@uc-biotech.pt.

This article contains supporting information online at www.pnas.org/lookup/suppl/doi:10.1073/pnas.1617451114/-/DCSupplemental.

www.pnas.org/cgi/doi/10.1073/pnas.1617451114

We established the conditions for the differentiation of hPSCs into embryonic ECs followed by their maturation under flow conditions for more accurate toxicological assessment. Using a high-throughput assay, we identified fluphenazine (an antipsychotic) and 7-cyclopentyl-5-(4-phenoxy)phenyl-7H-pyrrolo[2,3-d]pyrimidin-4-ylamine (7-Cyclo; an antiinflammatory agent) as compounds that interfere with cell viability and disrupt in vitro embryonic vascular networks. Our results further show that 7-Cyclo's effect is mediated by the inhibition of vascular endothelial growth factor receptor 2 (VEGFR2) highly expressed in the embryonic ECs. These findings were validated in vitro, where we demonstrated that 0.001 μM 7-Cyclo interferes with hPSC-derived EC cord-like structure in Matrigel and cell viability. Additionally, in vivo, we showed that 0.1 μM 7-Cyclo specifically blocks the motility and sprouting of arterial ECs during intersomitic vessel development in zebrafish embryos.

Results

Derivation of ECs from hPSCs. To differentiate human embryonic stem cells (hESCs) into ECs, we used a protocol that combined $VEGF_{165}$ (9), thymosin β4 (Tβ4) (10), and TGF-β inhibitor (SB431542) (11) as inductive agents of EC differentiation (Fig. 1*A*). We obtained ∼5% $CD31^+$ cells at 18 d of differentiation. To determine whether $CD31^+$ cells after 18 d of differentiation could differentiate into ECs, $CD31^+$ cells were isolated by using magnetic activated cell sorting (MACS) and cultured in EGM-2 medium supplemented with SB431542. Gene expression analysis in cells differentiated for three passages (between 18 and 22 d after cell seeding) indicated that the cells expressed *CD34*, vascular endothelial cadherin (*VECAD*), and *VEGFR2* at the same or at a higher level compared with human umbilical vein ECs (HUVECs), albeit they exhibited a lower expression of *VWF* and *CD31*, which may indicate different levels of maturation (Fig. 1*B*). Flow cytometry and immunocytochemistry analyses showed that $CD31^+$ cells cultured for three passages expressed high levels of EC markers (Fig. 1 *C* and *D*), but not other mesoderm-derived cell lineages, such as the smooth muscle cell marker α-SMA (*SI Appendix*, Fig. S1*A*). Similar results were obtained for ECs derived from human induced pluripotent stem cells (hiPSCs) generated from cord blood (12) (*SI Appendix*, Fig. S2). Microarray data from hESC-derived ECs, human umbilical artery ECs (HUAECs), human arterial ECs (HAECs), and HUVECs were integrated. Clustering analysis showed that hESC-derived ECs are more related to an arterial than a venous gene expression profile (*SI Appendix*, Fig. S1*B*). Overall, our results showed that we obtained a significantly pure EC population from hPSCs.

Next, we performed gene microarray for hESC-derived ECs, HUAECs (fetal cells), and HAECs (adult cells) and compared the global gene expression with data from ECs isolated from embryonic day 8.5 (E8.5) mouse embryos (13). Interestingly, the hESC-derived ECs showed a robust clustering to embryonic ECs (Fig. 1*E*). We then used *k*-means clustering to extract the set of genes enriched in both embryonic and hES-derived ECs (Fig. 1*E* and *SI Appendix*, Table S2). Thirteen genes were selected and confirmed by quantitative RT-PCR (qRT-PCR) (*DLL1*, *EPHB2*, *LYN*, *TEK*, *ID1, NRP2, CAST, FLT1, IGF1, DKK3, NIN, LEF1*, and *SORBS3*; Fig. 1*F* and *SI Appendix*, Fig. S1*C*). ECs isolated from embryonic mouse aorta at day E12.5 (mAECs E12.5) and postnatal day 1 (mAECs p1) were used to confirm the embryonic identity. qRT-PCR results validated the microarray analysis and further showed that the 13 genes were up-regulated in mAECs E12.5 compared with mAECs p1 (Fig. 1*F* and *SI Appendix*, Fig. S1*C*). Together, the results indicated that hESC-derived ECs have embryonic-like properties.

Next, we asked whether hESC-derived ECs are functional. hESC-derived ECs are able to take up Dil-labeled acetylated low-density lipoprotein and formed cord-like structures when cultured in the basement membrane Matrigel (Fig. 1*C*). In addition, hESC-derived ECs responded to the vasoactive agonists, similar to HUVECs or HUAECs, by increasing the intracellular levels of Ca^{2+} (Fig. 1*G*). hESC-derived ECs did not respond to thrombin as HUAECs, and they had different response profiles to $VEGF_{165}$, prostaglandin H2-analog, and histamine. No similarity was found in the response profiles of hESC-derived ECs and HUVECs. Furthermore, hESC-derived ECs responded to proinflammatory stimuli, such as tumor necrosis factor alpha (TNF-α), by increasing the expression of ICAM1, CD40, and VCAM1 (Fig. 1*H*). Together, our results show that hESC-derived ECs are functional; however, they show differences in their activity compared with HUAECs and HUVECs, which is likely due to their embryonic properties.

To induce the maturation of hESC-derived ECs, we cultured the cells under flow conditions (20 dyne/cm^2) for 7 d. Knowledge about flow conditions during human embryo development is scarce, and thus we selected arterial flow conditions (14) to culture the hESC-derived ECs that have a gene expression profile more related to arterial ECs (*SI Appendix*, Fig. S1*B*). Previous studies have shown that a mechanosensory complex formed by CD31, VECAD, and VEGFR2 mediates the responsiveness of ECs to flow shear stress (15). Indeed, the expression of CD31 and VEGFR2 was up-regulated in flow conditions (*SI Appendix*, Fig. S1 *D* and *E*), as previously shown in adult ECs (15). The maturation of the hESC-derived ECs was also evaluated by their capacity to express heparan sulfate proteoglycan (HSPG), a component of the glycocalyx layer (16) (*SI Appendix*, Fig. S1*F*). HSPG is absent in ECs cultured in static conditions, as shown in previous studies (16). However, both hESC-derived ECs and control HUAECs cultured under flow conditions were abundantly decorated with HSPGs. HSPGs are detected in the apical region of ECs (XZ view) exposed to flow. These results showed that hESC-derived ECs responded to flow by producing HSPG, as observed in vivo. Overall, our results indicated that hESC-derived ECs mature under flow conditions, as shown by the up-regulation of the mechanosensory complex and their capacity to express HSPG.

High-Throughput Identification of Compounds That Interfere with hESC-Derived EC Activity Followed by Hit Validation in Flow Conditions. To investigate whether hESC-derived ECs cultured under static and flow (20 dyne/cm^2) conditions can respond to compounds that interfere with EC activity, we cultured cells for 7 d in each condition, after which the culture medium was supplemented or not with terbinafine (0.1 and 1 μM), an antiangiogenic drug that suppresses EC proliferation and activates EC apoptosis (17, 18), for an additional day. Our results indicated that the hESC-derived ECs are highly sensitive to terbinafine because the expression of inflammation (*ICAM-1*; *E-SELECTIN*), oxidative stress sensing (*HO-1*), and vasculature modulation (*eNOS*) genes was up-regulated in cells cultured in flow conditions with terbinafine (*SI Appendix*, Fig. S3). In addition, the expression of dimethylarginine-dimethyl-amino-hydrolase (*DDAH*) genes, a family of enzymes that metabolizes asymmetric dimethylarginine (ADMA) (19), a marker of EC dysfunction, was significantly down-regulated in hESC-derived ECs cultured under flow conditions ($P < 0.05$ or 0.01; $n = 4$), but not in static conditions. Furthermore, the secretion of ADMA and the ratio of the von Willebrand factor propeptide (vWFpp):von Willebrand factor (vWF) (20), both indicators of EC activation/injury, were higher in hESC-derived ECs cultured in flow conditions in the presence of terbinafine than in static conditions. Overall, these studies demonstrate that hESC-derived ECs can be used to test inhibitory molecules, and cells cultured under physiologic shear stress have a higher sensitivity to terbinafine than cells cultured in static conditions.

Having demonstrated the drug sensitivity of hESC-derived ECs, we next asked whether we could identify compounds that interfered with embryonic-like ECs using high-throughput screening. Thus, we exposed hESC-derived ECs in static conditions to a Library of Pharmacologically Active Compounds (LOPAC) consisting of

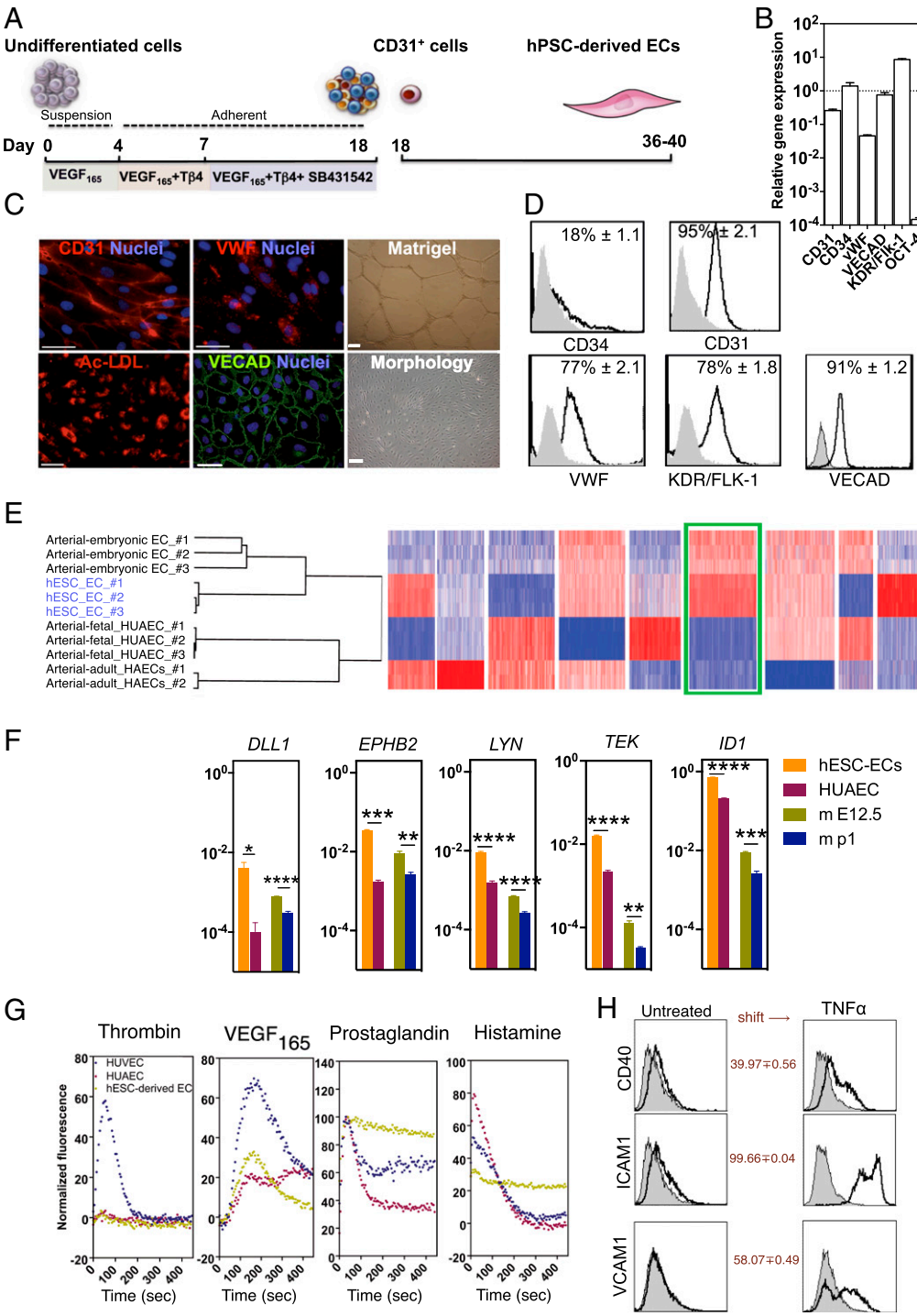

Fig. 1. Differentiation and properties of hESC-derived ECs. (*A*) Scheme illustrating the differentiation protocol. (*B*) Gene expression on hESC-derived ECs. hESC-derived ECs were obtained from CD31+ cells isolated by MACS and differentiated for three passages (~22 d after cell seeding). Gene expression was evaluated by qRT-PCR, and the values were normalized by the corresponding gene expression observed in HUVECs, except for OCT-4, which was normalized by the corresponding gene expression in undifferentiated hESCs. Results are mean ± SEM ($n = 4$). (*C*) Expression of EC proteins and functionality of hESC-derived ECs. (Scale bars: 50 μm.) (*D*) Flow cytometry analysis of hESC-derived ECs. Percentages of positive cells were calculated based on the isotype controls (gray plot) and are shown in each histogram plot. Results are mean ± SEM ($n = 3$). (*E*) Hierarchical clustering showing the integration of gene expression data from hESC-derived ECs (in blue) and mouse embryonic ECs (data from ref. 13). Our results show that hESC-derived ECs cluster with embryonic ECs more than fetal or adult arterial ECs. The heatmap displays 10 clusters of genes. The one highlighted in green is a cluster of genes enriched in embryonic and hESC-derived ECs (presented in *SI Appendix*). Red designates increased expression, and blue designates decreased expression relative to the mean. (*F*) qRT-PCR analysis for genes more highly expressed in embryonic ECs than in fetal or adult ECs. hESC-derived ECs at passage 4, HUAECs, embryonic mouse aortic ECs at day 12.5 (mAEC E12.5), and postnatal day 1 (mAEC p1) have been characterized. Gene expression was normalized by the expression of GAPDH. Results are mean ± SEM ($n = 4$). Statistical analyses were performed by an unpaired *t* test. $^{*}P < 0.05$; $^{**}P < 0.01$; $^{***}P < 0.001$; $^{****}P < 0.0001$. (*G*) Variation of intracellular Ca^{2+} in FURA-2–loaded cultured hESC-derived ECs, HUAECs, or HUVECs in response to several agonists. Traces are representative of six independent experiments for each condition. (*H*) hESC-derived EC activation by exposure to TNF-α (10 ng/mL) for 24 h. The shift in each plot indicates the percentage of cells that express a specific marker after exposure to TNF-α, subtracted by the percentage of cells that express the corresponding marker in the absence of TNF-α. Results are mean ± SEM ($n = 4$).

1,280 bioactive compounds, and we assessed cell viability after 4 d using a PrestoBlue assay (resazurin-based solution that is reduced by viable cells) (Fig. 2*A*). The library was screened at a single concentration (4.5 μM) according to previous studies using ECs (21–24) and other cells (25, 26), in a volume of 200 μL per well of EGM-2 medium containing 0.25% DMSO (vol/vol). To identify compounds that selectively target ECs, we screened the same library against human anterior cruciate ligament (ACL) cells. These cells were chosen because they are nonvascular cells isolated from a poorly vascularized tissue, and thus their survival does not heavily rely on blood supply (27). Of the 1,280 compounds, 99 compounds induced differences in cell viability (hESC-derived ECs vs. ACL cells) of >50% and were considered for further analyses (*SI Appendix*, Table S3). To identify compounds that were selective to embryonic ECs, but not fetal ECs, we screened the library against HUAECs (Fig. 2*A*). Six compounds (danazol, chlorpromazine hydrochloride, ellipticine, 3′,4′-dichlorobenzamil, fluphenazine dihydrochloride, and 7-Cyclo) affected cell viability in both cells by a difference of 20% (Fig. 2*B*). The compounds selected from the primary screen were then tested against hESC-derived ECs and HUAECs at different concentrations to obtain a dose–response curve (Fig. 2*C* and *SI Appendix*, Fig. S4). Compounds 7-Cyclo and fluphenazine dihydrochloride were selected for further testing due to the significant difference in the effects on hESC-derived ECs vs. HUAECs.

To test the properties of 7-Cyclo and fluphenazine hydrochloride in the disruption of vascular networks, microvessels of hESC-derived ECs and HUAECs were formed on top of Matrigel to have a patent lumen (*SI Appendix*, Fig. S5) and subsequently exposed to the drug between 3 and 20 h (depending on the assay). Our results showed that there was a statistically significant reduction in the network length and number of sprouts in microvessels formed by hESC-derived ECs after incubation with 1 μM 7-Cyclo, whereas a negligible effect was observed in microvessels formed by HUAECs (Fig. 3 *A* and *B* and *SI Appendix*, Fig. S6*A*). Importantly, the toxicity of 7-Cyclo against hESC-derived ECs was extensive to 0.001 μM (*SI Appendix*, Fig. S7*A*). A similar trend was observed for cells treated with fluphenazine, although less pronounced than 7-Cyclo (Fig. 3*C* and *SI Appendix*, Fig. S6*B*).

We complemented these results by evaluating cell metabolism as well as cell viability by annexin V/propidium iodide (PI) staining in hESC-derived ECs and HUAECs cultured on top of Matrigel. Our results show that hESC-derived ECs reduce significantly ATP production and have significant apoptosis/necrosis when cultured with 7-Cyclo in concentrations up to 0.001 μM for 3 h (Fig. 3 *D* and *E* and *SI Appendix*, Fig. S7*B*). This effect was less pronounced in HUAECs cultured with 7-Cyclo. In addition, the higher toxicity of 7-Cyclo (1 μM) against human embryonic ECs compared with fetal ECs was also confirmed in mouse ECs, specifically mAECs E12.5 against mAECs p1 (*SI Appendix*, Fig. S8). Moreover, hESC-derived ECs were more sensitive to the toxicity effects of fluphenazine than HUAECs, although the effect in both cells was relatively lower than that observed for 7-Cyclo (Fig. 3 *F* and *G*).

Fluphenazine has been described as an antipsychotic agent that inhibits calmodulin in ECs and increases intracellular concentration of Ca^{2+} (28). The inhibition of calmodulin leads to the inhibition of calmodulin kinase II, which, in turn, inhibits the phosphorylation of extracellular signal-regulated kinase (ERK) (29) and finally affects cell survival. Our results indicate that embryonic ECs cultured with fluphenazine showed higher mobilization of intracellular levels of Ca^{2+} (*SI Appendix*, Fig. S9), lower calmodulin kinase II activity, and lower levels of ERK and AKT phosphorylation than postnatal ECs (*SI Appendix*, Fig. S10). For further testing, we selected 7-Cyclo because hESC-derived ECs were more susceptible to this compound than fluphenazine.

To evaluate the effects of 7-Cyclo in flow conditions, hESC-derived ECs were cultured in a poly(dimethylsiloxane) (PDMS) microfluidic system with cylindrical channels for 7 d at 20 dyne/cm^2 (Fig. 4*A*). ECs were able to form a confluent monolayer on the entire inner surface of the channel after 48 h. At day 7, cells were exposed to EGM-2 medium supplemented with 1 μM 7-Cyclo for 24 h, and their gene expression and secretome were analyzed

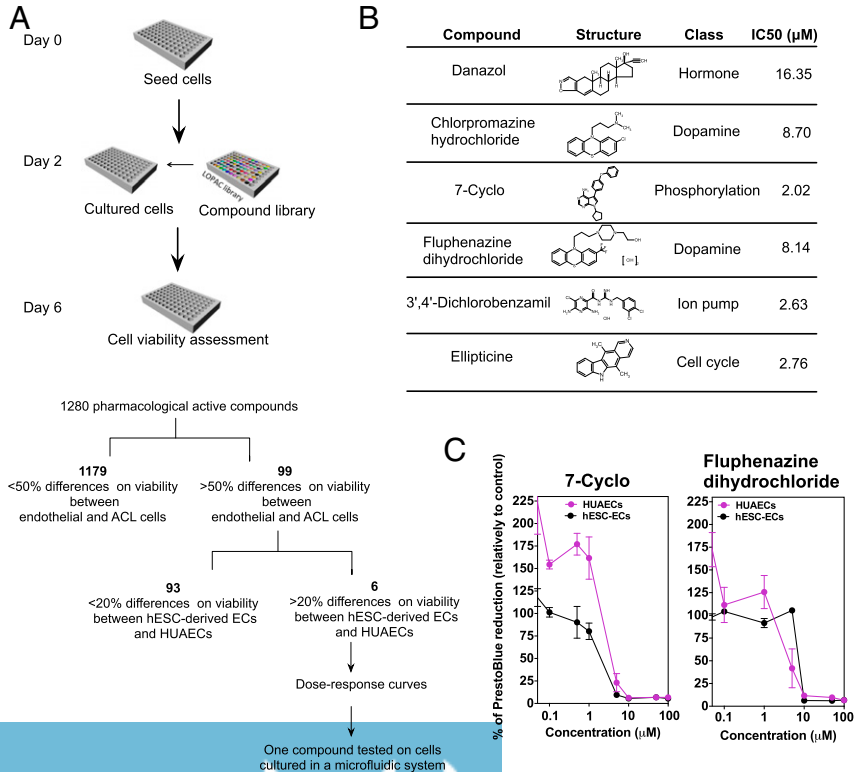

Fig. 2. High-throughput screening (HTS) to identify compounds that interfere with hESC-derived ECs. (*A*) Schematic representation of the HTS assay. (*B*) Small molecules identified after the analysis of the primary screen. The hits have preferential cytotoxicity against hESC-derived ECs. IC_{50} values are for hESC-derived ECs. (*C*) Dose–response curve for HUAECs and hESC-derived ECs exposed to 7-Cyclo and fluphenazine. Values are normalized against nontreated cells (control). Results are mean ± SEM ($n = 4$).

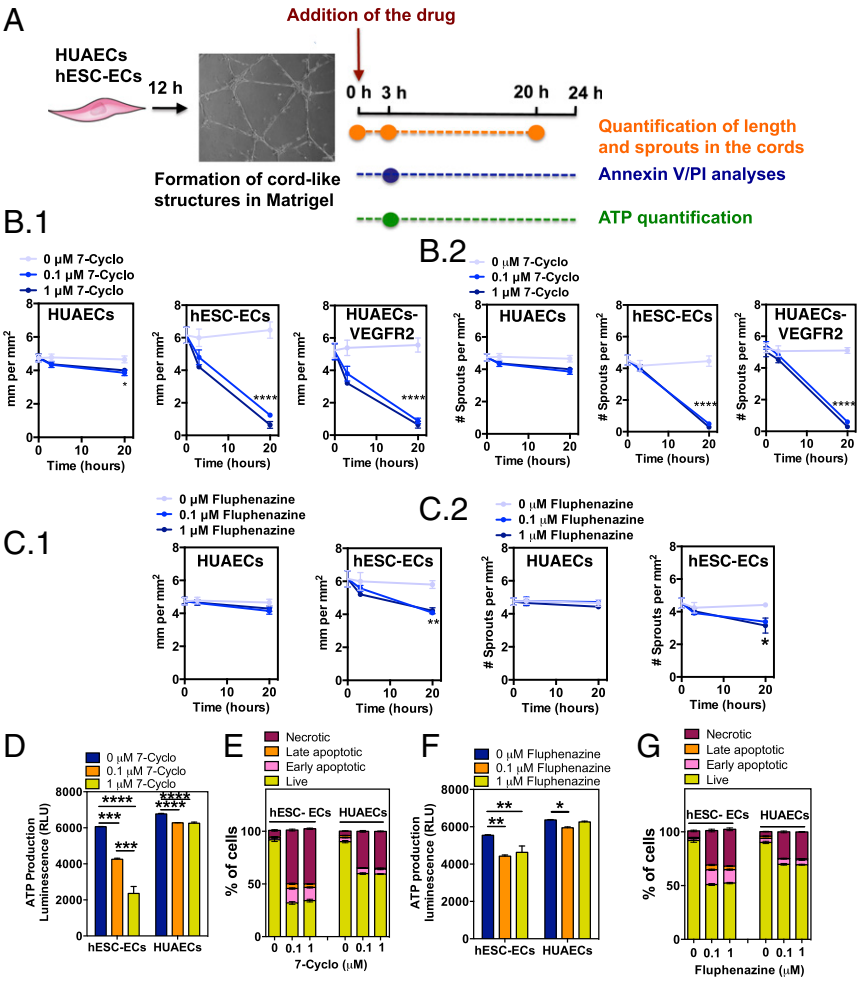

Fig. 3. Effect of 7-Cyclo and fluphenazine in angiogenesis, cell survival, and metabolism. (*A*) Secondary assays to show the preferential effect of 7-Cyclo in hESC-derived ECs than HUAECs. (*B* and *C*) Quantification of length (*B1* and *C1*) and sprouts (*B2* and *C2*) of cord-like structures in hESC-derived ECs, HUAECs, or HUAECs overexpressing VEGFR2 cultured on top of Matrigel for 12 h and then exposed for 0, 3, and 20 h to 7-Cyclo (*B*) or fluphenazine (*C*). Results are mean ± SEM ($n = 4$; two phase-contrast images per well and time). In *B* and *C*, statistical analyses between experimental groups and no treatment (0 μM 7-Cyclo) for the same time were performed by a one-way ANOVA test followed by a Newman–Keuls multiple comparisons test. (*D* and *F*) ATP analyses on hESC-derived ECs or HUAECs cultured on top of Matrigel for 12 h and then exposed for 3 h to 7-Cyclo (*D*) or fluphenazine (*F*). Results are mean ± SEM ($n = 4$). Statistical analyses were performed by one-way ANOVA test followed by a Newman–Keuls multiple comparisons test. (*E* and *G*) Quantification by flow cytometry of cell viability (annexin−/PI−), necrosis (annexin−/PI+), early (annexin+/PI−), and late (annexin+/PI+) apoptosis by using annexin V/PI staining, in cells cultured on top of Matrigel for 12 h and then exposed for 3 h to 7-Cyclo (*E*) or fluphenazine (*G*). Results are mean ± SEM, $n = 4$. *$P < 0.05$; **$P < 0.01$; ***$P < 0.001$; ****$P < 0.0001$.

(Fig. 4*B*). Our results revealed that hESC-derived ECs showed significant cell death (*SI Appendix*, Fig. S11*A*). In addition, hESC-derived ECs exposed to 7-Cyclo expressed significantly higher levels of inflammatory genes, such as *ICAM-1*, *E-SELECTIN*, *HO-1*, and *eNOS* ($P < 0.0001$, $n = 4$), and expressed lower levels of *DDAH1* and *DDAH2* ($P < 0.05$ or 0.0001, $n = 4$), which are enzymes that metabolize ADMA, compared with cells cultured under static conditions (Fig. 4*C*). Interestingly, EC inflammation and injury occurred upstream of cell apoptosis/necrosis (*SI Appendix*, Fig. S11*B*). In the case of HUAECs cultured under the same conditions, the effect was less pronounced. No down-regulation of *DDAH-1* and *-2* was observed. We complemented these gene analyses with analyses of ADMA and the ratio of vWFpp:von vWF secreted by these cells (Fig. 4*D*). hESC-derived ECs or HUAECs cultured in static conditions in the presence of the drug demonstrated similar secretion of ADMA or vWFpp:vWF as control conditions (i.e., without the drug). Importantly, hESC-derived ECs cultured under flow conditions in the presence of 7-Cyclo secreted higher levels of ADMA (2.5-fold) and vWFpp:vWF (1.6-fold) than without the drug, and significantly higher levels of ADMA were observed compared with HUAECs. This result was likely due to differences in the expression profile of 7-Cyclo molecular targets (i.e., tyrosine kinases; see below) either in static or flow conditions (*SI Appendix*, Fig. S12). Overall, our results indicated that hESC-derived ECs were more sensitive to the effects of 7-Cyclo compared with HUAECs.

To further confirm the effects of 7-Cyclo in the embryonic vasculature, we incubated mAECs E12.5 and mAECs p1 with 7-Cyclo (1 μM) for 24 h under static conditions. Inflammation, oxidative stress sensing, vascular modulation, and vascular injury-sensing genes were statistically up-regulated in mAECs E12.5 compared with cells without treatment (*SI Appendix*, Fig. S13). In contrast, 7-Cyclo had no effect on mAECs p1. The degree of action of 7-Cyclo in mAECs E12.5 was similar to the effect identified in hESC-derived ECs (Fig. 4*C*).

We further validated these findings in vivo using zebrafish Tg(fli1a:eGFP)^{y1} embryos (30) by evaluating the effect of 7-Cyclo on the development of intersegmental blood vessels (ISVs). The 7-Cyclo was added to the water of 22–23 h postfertilization (hpf) embryos at a concentration of 0, 0.1, 1, and 10 μM for 8 h, and

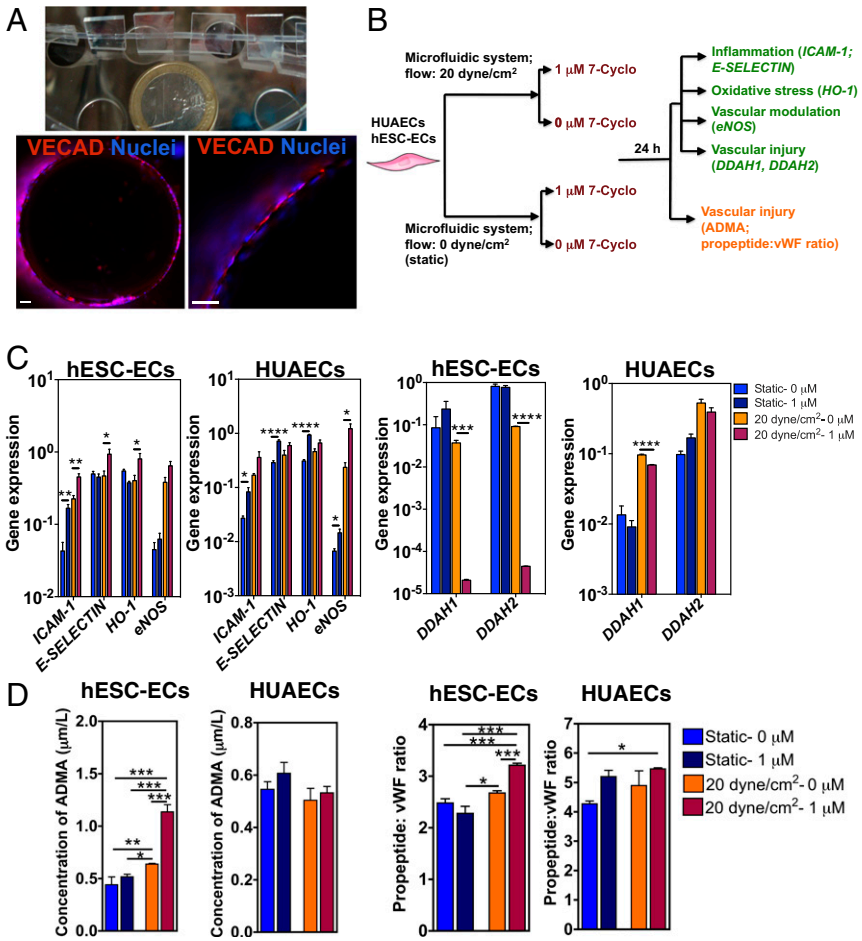

Fig. 4. Effect of 7-Cyclo in flow conditions. (*A*) Macroscopic view of the PDMS microfluidic system (the microchannels have a diameter of 900 μm and an average length of 0.5 cm) and fluorescent images of microchannel cross-sections showing that ECs can grow in the inner surface of the microfluidic channel after 48 h and be stable for at least 7 d at 20 dyne/cm2. (Scale bars: 50 μm.) (*B*) Schematic representation of the experiments performed to evaluate the effect of 7-Cyclo in ECs cultured under flow or static conditions. (*C*) Expression of genes involved in inflammation (ICAM-1; E-SELECTIN), oxidative stress sensing (HO-1), vascular modulation (eNOS), and vascular injury sensing (DDAH1 and DDAH2) in hESC-derived ECs and HUAECs after 24 h of incubation with 0 or 1 μM 7-Cyclo. Results are mean ± SEM ($n = 4$). Statistical analyses between groups at static or flow conditions were performed by an unpaired *t* test. (*D*) Quantification of ADMA and vWFpp:vWF by ELISA in hESC-derived ECs and HUAECs after 24 h incubation with 1 μM 7-Cyclo. Results are mean ± SEM ($n = 6$). Statistical analyses were performed by one-way ANOVA test followed by a Newman–Keuls multiple comparisons test. *$P < 0.05$; **$P < 0.01$; ***$P < 0.001$; ****$P < 0.0001$.

(*i*) the number of ISVs, (*ii*) number of ISVs reaching the dorsal longitudinal anastomotic vessel (DLAV), and (*iii*) percentage of caudal plexus sprouts was quantified (Fig. 5 *A* and *B*). Our results show that 7-Cyclo is toxic to zebrafish embryos at a concentration of 0.1–1 μM. At concentrations of 1 μM, 7-Cyclo blocked the motility and sprouting behavior of arterial ECs during intersomitic vessel development in zebrafish embryos. We also evaluated the effect of 7-Cyclo in adult zebrafish Tg(fli1a:eGFP)^{y1}. Because drug accessibility and pharmacokinetics is likely different in both models (31), the concentration and time of exposure of 7-Cyclo will be different, making a direct comparison difficult. To overcome this issue, we evaluated the effect of 7-Cyclo on the zebrafish caudal fin regeneration model (*SI Appendix*, Fig. S14). In this model, we could monitor simultaneously the effect of 7-Cyclo in the preformed vasculature (mature ECs) and in the forming vasculature [immature ECs; more dependent in VEGF signaling than preformed vasculature (31)]. The zebrafish tail fin is very thin and optically transparent, which facilitates the vascular toxicity monitoring. Our results clearly show a more dramatic effect of the drug on newly formed vessels than on the preexistent vessels in the adult.

Effect of 7-Cyclo in Embryonic ECs. The 7-Cyclo is a cell-permeable pyrrolopyrimidine that acts as a potent inhibitor of tyrosine kinases (32). To understand the distinct effect of 7-Cyclo in embryonic vs. fetal/adult ECs, we mined the microarray data and compared the expression levels of different kinases. Of the 38 genes that encode for tyrosine kinases (Fig. 5*D* and *SI Appendix*, Table S4), 13 of the genes (*EFS*, *VEGFR2*, *LYN*, *EGFR*, *ZAP70*, *FLT1*, *FLT4*, *LTK*, *MERTK*, *NRP1*, *NTRK2*, *TEK*, and *TYRO3*) were expressed at higher levels in hESC-derived ECs compared to HUAECs or HEACs. The expression of *EFS*, *VEGFR2*, *LYN*, *EGFR*, *ZAP70*, *NRP1*, and *TEK* was further confirmed by using qRT-PCR (Fig. 5*C*).

Next, we evaluated the expression of tyrosine kinase genes on mAECs E12.5 and p1 to validate the results obtained in hESC-derived ECs. The same results were observed—that is, tyrosine kinases were expressed more in embryonic ECs (in human and mouse) compared with fetal/adult tissues [except for *EGFR* in mouse (*Egfr*)]. The kinase activity of hESC-derived ECs and HUAECs was assessed by using luminescence (signal is inversely correlated with the level of kinase activity) in the absence or presence of compound 7-Cyclo (Fig. 5*E*). After 24 h of incubation with 7-Cyclo (0.1 or 1 μM), the kinase activity of hESC-derived ECs decreased significantly from time 0 ($P < 0.01$), whereas no significant decrease was observed in HUAECs.

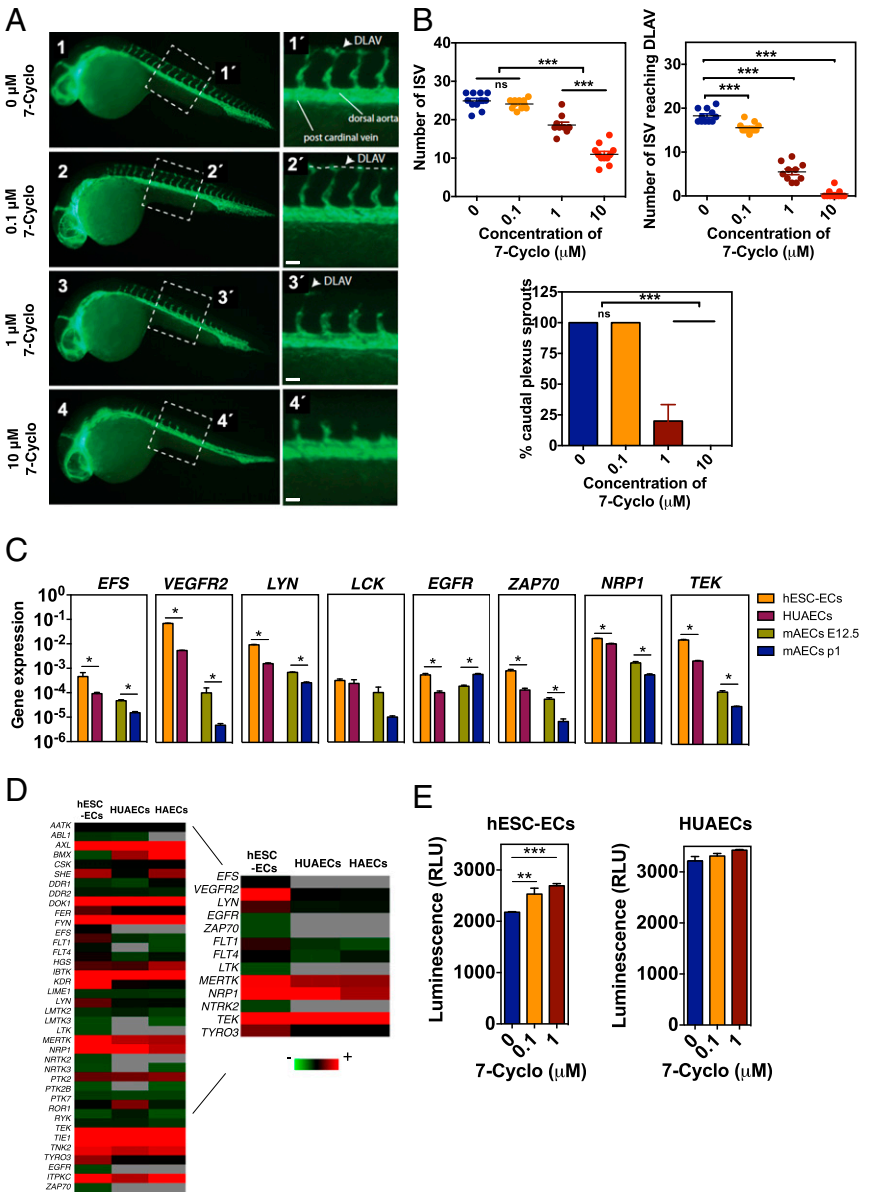

Fig. 5. Effect of 7-Cyclo in zebrafish embryos and molecular targets. (*A*) Effect of 7-Cyclo on zebrafish embryos. Tg(fli1a:EGFP)y1 *Danio rerio* were incubated for 8 h at the concentrations shown (*A1–A4*) and starting at 22–23 hpf. *Insets* show the effect of 7-Cyclo in ISVs reaching the DLAV (arrowheads). (Scale bars: 100 µm.) (*B*) Embryos were scored for the number of ISVs along the anterior–posterior axis, the number of ISV's that reach the DLAV, and for the presence or absence of sprouts at the caudal plexus. Ten or more embryos were tested per experimental group per independent experiment (total of three independent experiments). The data shown are representative of one of three independent experiments. Statistical analyses were performed by one-way ANOVA test followed by a Bonferroni multiple comparisons test. (*C*) Expression of tyrosine kinases by qRT-PCR. Gene expression was normalized by the expression of GAPDH. Results are mean ± SEM ($n = 4$). Statistical analyses were performed by a Mann–Whitney test. (*D*) Microarray analysis showing the expression of tyrosine kinases in hESC-derived ECs, HUAECs, and HAECs. The list of genes is linked to the heatmap. Some of the tyrosine kinases are more highly expressed in hESC-derived ECs than in HUAECs or HAECs (displayed in the zoom of the microarray). (*E*) Kinase activity on hESC-derived ECs and HUAECs after incubation with variable concentrations of 7-Cyclo. Luminescence is inversely related to kinase activity. Results are mean ± SEM ($n = 6$). Statistical analyses were performed by one-way ANOVA test followed by a Newman–Keuls multiple comparisons test. *$P < 0.05$; **$P < 0.01$; ***$P < 0.001$. ns, not significant.

Together, our results indicate that 7-Cyclo affects hESC-derived ECs, which likely inhibits tyrosine kinases that are highly expressed in the embryonic state.

VEGFR2 is an important target of 7-Cyclo because the IC_{50} of the drug for this tyrosine kinase is 1.57 µM (33). Therefore, we evaluated the effect of the drug in the phosphorylation of VEGFR2. The phosphorylation decreased significantly in hESC-derived cells, but not in HUAECs (Fig. 6*A*). However, if we overexpressed VEGFR2 in HUAECs (*SI Appendix*, Fig. S15), we had a significant decrease in VEGFR2 phosphorylation (Fig. 6*A*), as well as in the length and sprouts of cord-like vessels formed on Matrigel (Fig. 3*B*). Like in the human system, in the mouse system the phosphorylation decreased in mAEC E12.5, but not in mAECs p1, indicating that embryonic ECs are more sensitive to 7-Cyclo than postnatal ECs (Fig. 6*A*). Our results further showed that the increased sensitivity of embryonic ECs to 7-Cyclo is likely due to their higher expression of VEGFR2 (hESC-ECs: 76.5 ± 2.9; mAEC E12.5: 67.3 ± 3.1) compared with postnatal ECs (HUAECs: 70.4 ± 2.1; mAECs p1: 49.6 ± 2.6) (Fig. 6*B*). The increased sensitivity of embryonic ECs to 7-Cyclo is not due to

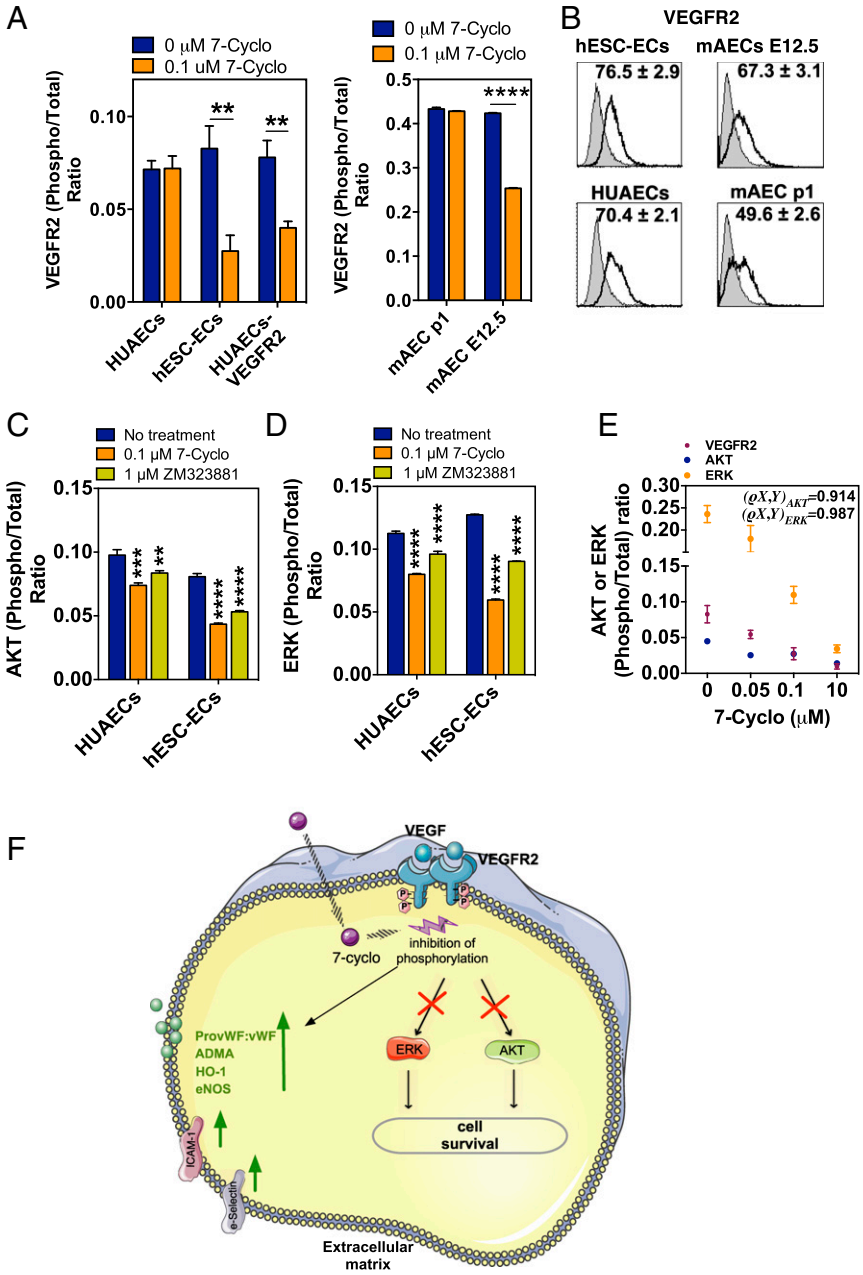

Fig. 6. Effect of 7-Cyclo in VEGFR2. (*A*) Phosphorylation of VEGR2 in human and mouse embryonic and postnatal cells treated with 0 or 0.1 μM 7-Cyclo for 72 h (by ELISA). Results were normalized by the total form of protein and indicate mean ± SEM ($n = 4$). HUAECs-VEGFR2 cells are HUAECs overexpressing VEGFR2. Statistical analyses between groups were performed by an unpaired *t* test. (*B*) VEGFR2 is more highly expressed in embryonic cells (hESC-ECs or mAECs E12.5) than in postnatal cells (HUAECs or mAECs p1), either in human or mouse cells. Percent of positive cells was calculated based on the isotype controls (gray plot) and is shown in the histogram plots. Values in histogram plots indicate mean ± SEM ($n = 3$). (*C* and *D*) Effect of 7-Cyclo (0.1 M) and ZM323881 (1 M; VEGFR2-specific inhibitor) in the phosphorylation of AKT (*C*) and ERK (*D*) in hESC-derived ECs and HUAECs for 15 min (by ELISA). Results were normalized by the total form of protein and indicate mean ± SEM ($n = 4$). Statistical analyses between experimental group "no-treatment" and the other two groups was performed by one-way ANOVA test followed by a Newman–Keuls multiple comparisons test. (*E*) Correlation between the inhibition of VEGFR2 phosphorylation and the inhibition of AKT ($P = 0.914$) or ERK ($P = 0.987$) phosphorylation. Correlations indicate a strong relationship between both events. Values indicate mean ± SEM ($n = 4$). (*F*) Schematic representation of the impact of 7-Cyclo in embryonic ECs. The 7-Cyclo inhibits VEGFR2 phosphorylation, leading to the inhibition of downstream pathways involved in cell proliferation and survival (ERK and AKT pathways). The 7-Cyclo also increases the expression of the molecules involved in vascular injury such as ADMA, propeptide vWF, eNOS, ICAM-1, eSelectin, and HO-1. *$P < 0.05$; **$P < 0.01$; ***$P < 0.001$; ****$P < 0.0001$.

changes in the level of VEGF expression after drug exposure (*SI Appendix*, Fig. S16).

Downstream effectors of VEGFR2 are ERK and AKT signaling pathways (34). Phosphorylation of ERK activates cell proliferation, while phosphorylation of AKT activates cell proliferation, migration, and survival (34, 35). Like ZM323881, a highly selective inhibitor of VEGFR2 (34), 7-Cyclo reduced significantly the phosphorylation of both AKT and ERK in hESC-ECs (Fig. 6 *C* and *D*). This effect was significantly lower in HUAECs. To determine whether the inhibition of AKT and ERK was synchronized with VEGFR2 inhibition, we performed dose-effect analyses and calculated the correlation between the

slopes of both graphs (Fig. 6*E*). The correlations found (AKT: 0.914; ERK: 0.987) indicate that there is a strong relationship between AKT and ERK inhibition and VEGFR2 blocking by 7-Cyclo. Together, our results indicate that 7-Cyclo inhibits the kinase activity of VEGFR2, which further inhibits AKT and ERK signaling pathways, inducing cell death (Fig. 6*F*). The higher sensitivity of embryonic ECs to 7-Cyclo than postnatal ECs is likely due to high expression of VEGFR2.

Discussion

In this study, we described a platform for the high-throughput screening of chemicals that affect embryonic vascular development. This platform includes (*i*) the differentiation of hPSCs into embryonic-like ECs, followed by their maturation under flow shear stress; (*ii*) high-throughput identification of small molecules that interfered with embryonic-like EC survival in a two-step protocol; (*iii*) confirmation of the hits in embryonic-like ECs cultured under flow shear stress; and (*iv*) final validation in mouse embryonic ECs and the zebrafish animal model.

Previous studies have performed very useful in vivo screens for inhibitors of vascular development in zebrafish embryos (36) and *Xenopus* embryos (37). Although in vivo screening systems integrate all physiological processes, they have some limitations that can be addressed by high-throughput cellular platforms. First, the identified compounds might affect embryonic as well as fetal/adult vasculature. In the present work, we identified drugs that more specifically target embryonic ECs using a two-step protocol involving (*i*) a primary screen against a nonvascular cell (ligament cells) and (*ii*) a primary screen against fetal ECs (HUAECs). Second, in the in vivo testing, the test compounds did not have direct access to their target, but were metabolized or resorbed. In addition, other cell types or the immune system can alter the drug effects, which makes difficult to attribute the primary target for the drug (21). Third, studies in animal embryos (zebrafish, *Xenopus*, rats, and rabbits) do not account for differences in the vascular development between humans and small animals (4).

Recent studies have shown the derivation of ECs from hPSCs with high efficiency in chemical defined medium (38, 39) and exhibiting features of arterial-like ECs (39–42); however, it was unclear what their maturation stage was under flow conditions and whether they exhibited embryonic or adult features. Both features have significant impact on drug screening, as confirmed by results of the present work. In this study, we derived embryonic-like ECs. At the gene level, clustering analyses showed that hESC-derived ECs were more related to embryonic than adult ECs. Although a defined set of embryonic EC gene markers has not yet been identified, in this study, we identified 328 embryonic EC genes, some of which were validated by qRT-PCR (*DLL1*, *EPHB2*, *LYN*, *TEK*, *ID1, NRP2, CAST, FLT1, IGF1, DKK3, NIN, LEF1*, and *SORBS3*). We further showed that embryonic ECs have a high expression of tyrosine kinases, including *EFS*, *VEGFR2*, *LYN*, *EGFR*, *ZAP70*, *NRP1*, and *TEK*. Importantly, flow shear stress enhanced the maturation of ECs as shown by an up-regulation of EC mechanosensory complex proteins VECAD and VEGFR2, cell alignment in the direction of the flow, and production of HSPGs.

There is currently a limited set of chemical compounds that have been described to affect human embryonic vascular development. Thalidomide, which was prescribed in the 1960s, is the most well-known embryonic vascular disruptive drug. Thalidomide inhibits angiogenesis via the prevention of filopodial extensions from the endothelial tip cell (43). Thalidomide is one of the drugs of the LOPAC; however, the drug was not a hit in our screening. This finding was likely due to the high concentration of the drug (>5 μM) that is required to affect cell viability, as previously shown (44).

In the present study, the screening of the chemical library was performed at one concentration (4.5 μM), and the endpoint was cell viability after 96 h of exposure. This endpoint may reflect multiple effects of the selected drug, and thus we further confirmed its toxicity in multiple secondary assays for low concentrations of the drug (up to 0.001 μM). Although not explored, the effect of the chemical library in specific properties of ECs, such as migration, capillary tube formation, vascular inflammation, among others (24), may also be important for the identification of drugs affecting embryonic vascular development. The concentration selected for the screening was based on previous screenings (21, 22, 24) and was below the toxicity of thalidomide (>5 μM) (44).

In recent years, several drugs have been identified to disrupt vascular development in zebrafish and *Xenopus* embryos (36, 37, 45); however, in many cases, the drugs have not been validated in human cells, and most of the drugs likely affect both the adult vascular system and embryonic vascular development. In this study, we identified two embryonic EC inhibitors, namely, fluphenazine and 7-Cyclo, using high-throughput screening. Fluphenazine medication is not recommended during pregnancy; however, for a woman who is taking this medication at the time of conception, by the time the pregnancy is confirmed, most or all of the organogenesis has already occurred. An international epidemiological survey of drug use in pregnancy showed that 3.5% of the women took psychotropic drugs during pregnancy (46). It was found that the human fetus exposed to fluphenazine had severe rhinorrhea, respiratory distress, and delayed extrapyramidal symptoms (47). Our study shows that fluphenazine has a higher effect in the disruption of embryonic vascular networks than postnatal ones.

Previous studies have demonstrated that 7-Cyclo (20 μM) disrupts blood vessel formation in *Xenopus* embryos and is an inhibitor of in vitro lymphangiogenesis (21, 37). Our results indicated that hESC-derived ECs exposed to medium supplemented with 7-Cyclo (1 μM) for 24 h under flow conditions showed an up-regulation of inflammatory genes and secretion of vascular injury markers. This effect was higher on hESC-derived ECs compared with HUAECs. Similar results were also obtained for mouse embryonic ECs and postnatal ECs (i.e., mouse embryonic ECs were sensitive to the toxicity of 7-Cyclo, whereas postnatal ECs showed no measurable effect against the same compound). We also confirmed in vivo the effect of 7-Cyclo on ISV development of zebrafish embryos and showed that it specifically blocked the motility and sprouting behavior of arterial ECs.

The effect of 7-Cyclo against embryonic-like ECs involved the inhibition of VEGFR2, which is highly expressed in embryonic ECs compared with fetal or adult ECs. This inhibition (at 0.1 μM) occurred in embryonic ECs (hESC-ECs), but not in fetal ECs (HUAECs), due to the high level of VEGFR2 expression in the former. However, the overexpression of VEGFR2 in HUAECs makes these cells sensitive to 0.1 μM 7-Cyclo. The inhibition of VEGFR2 leads to a significant inhibition of AKT and ERK pathways with higher efficiency than a commercial inhibitor. This inhibition, in turn, leads to cell necrosis. In conclusion, the platform described in this study is promising for the identification of compounds that affect vascular development, as well as to study embryonic vascular biology.

Methods

Detailed methods are available in *SI Appendix, SI Materials and Methods*.

hPSC Culture and Differentiation. Undifferentiated hESCs (passages 33–36; H9, WiCell) or hiPSCs K2 (passages 32–35; cord blood-derived iPSCs kindly donated by Ulrich Martin; Leibniz Research Laboratories for Biotechnology and Artificial Organs, Department of Cardiothoracic, Transplantation and Vascular Surgery, Hannover Medical School, Hannover, Germany) were grown on an inactivated mouse embryonic fibroblast feeder layer, as described (9, 48). Cells were induced to differentiate into ECs by using different protocols (*SI Appendix, SI Materials and Methods*). hESCs were used with the approval of the ethics commitee from University of Coimbra.

Isolation of CD31$^+$ Cells. CD31$^+$ cells were isolated from differentiated hESCs or hiPSCs at day 18 by using MACS (Miltenyi Biotec). Isolated cells were grown

on Petri dishes (1.5×10^4 cells per cm^2) coated with 0.1% gelatin and containing EGM-2 (Lonza) supplemented with SB431542 (10 μM). The methodologies for cell culture under flow conditions and cell characterization at gene, protein, and functional levels are provided in *SI Appendix, SI Materials and Methods*.

Human and Mouse Primary Cells. HUAECs and HUVECs were acquired from Lonza. mAECs E12.5 and mAECs p1 were isolated from mice cultured for 2–3 d in vitro in EC medium and immediately used. The cells were obtained from Innoprot.

Gene Expression Analyses (Microarray and qRT-PCR), Kinase Activity Quantification, Phosphorylation of AKT/ERK/VEGFR2, Matrigel Assays, Cell Viability Assays, and Intracellular Ca^{2+} Analyses. The methods are found in *SI Appendix, SI Materials and Methods*.

Evaluation of the Levels of Vascular Injury by Specific Markers. ELISA kits for vWF and vWFpp (Gen-Probe GTI Diagnostic) and ADMA (Enzo Life Sciences) were used to analyze supernatants collected from the shear stress experiments, according to manufacturer's recommendations.

High-Throughput Screening. The LOPAC (Sigma-Aldrich) was used to screen compounds that interfere with embryonic ECs. The compounds were solubilized in DMSO, and the final concentration used in the screen was 4.5 μM in a final volume of 200 μL per well (96-well plate). After 4 d of incubation, HUAEC or hESC-derived EC viability was assessed by using a PrestoBlue (Invitrogen) assay.

Zebrafish Line and Treatment with 7-Cyclo. Zebrafish Tg(fli1a:eGFP)^{y1} embryos (30) were used to evaluate the effect of 7-Cyclo on ISV development. The protocol is described in *SI Appendix, SI Materials and Methods*.

Statistical Analysis. An unpaired *t* test or one-way ANOVA with Newman–Keuls posttest was performed for statistical tests using GraphPad Prism software. Results were considered significant when $P < 0.05$.

ACKNOWLEDGMENTS. This work was supported by FEDER through the Program COMPETE and by Portuguese funding through FCT in context of the projects PTDC/SA-BEB/098468/2008, PTDC/SAU-TOX/121887/2010, and MITP-TB/ECE/0013/2013. The work was also supported by COMPETE in the context of Project "Stem-Cell Based Platforms for Regenerative and Therapeutic Medicine" (Centro-07-ST24-FEDER-002008). H.V. was supported by FCT for BD and BPD Fellowships SFRH/BD/40077/2007 and SFRH/BPD/87039/2012.

1. Makris SL, et al. (2011) Current and future needs for developmental toxicity testing. *Birth Defects Res B Dev Reprod Toxicol* 92(5):384–394.
2. Vasvari G, Dyckhoff G, Herold-Mende C (2005) Thalidomide protects endothelial cells from doxorubicin-induced apoptosis but alters cell morphology—a rebuttal. *J Thromb Haemost* 3(4):816–817, author reply 817–818.
3. Knudsen TB, Kleinstreuer NC (2011) Disruption of embryonic vascular development in predictive toxicology. *Birth Defects Res C Embryo Today* 93(4):312–323.
4. Kleinstreuer NC, et al. (2011) Environmental impact on vascular development predicted by high-throughput screening. *Environ Health Perspect* 119(11):1596–1603.
5. Mellin GW, Katzenstein M (1962) The saga of thalidomide. Neuropathy to embryopathy, with case reports of congenital anomalies. *N Engl J Med* 267:1184–92.
6. Tideman E, Marsál K, Ley D (2007) Cognitive function in young adults following intrauterine growth restriction with abnormal fetal aortic blood flow. *Ultrasound Obstet Gynecol* 29(6):614–618.
7. Levenberg S, Zoldan J, Basevitch Y, Langer R (2007) Endothelial potential of human embryonic stem cells. *Blood* 110(3):806–814.
8. Fiddes LK, et al. (2010) A circular cross-section PDMS microfluidics system for replication of cardiovascular flow conditions. *Biomaterials* 31(13):3459–3464.
9. Ferreira LS, et al. (2007) Vascular progenitor cells isolated from human embryonic stem cells give rise to endothelial and smooth muscle like cells and form vascular networks in vivo. *Circ Res* 101(3):286–294.
10. Smart N, et al. (2007) Thymosin beta4 induces adult epicardial progenitor mobilization and neovascularization. *Nature* 445(7124):177–182.
11. James D, et al. (2010) Expansion and maintenance of human embryonic stem cell-derived endothelial cells by TGFbeta inhibition is Id1 dependent. *Nat Biotechnol* 28(2):161–166.
12. Haase A, et al. (2009) Generation of induced pluripotent stem cells from human cord blood. *Cell Stem Cell* 5(4):434–441.
13. Swiers G, et al. (2013) Early dynamic fate changes in haemogenic endothelium characterized at the single-cell level. *Nat Commun* 4:2924.
14. Malek AM, Alper SL, Izumo S (1999) Hemodynamic shear stress and its role in atherosclerosis. *JAMA* 282(21):2035–2042.
15. Tzima E, et al. (2005) A mechanosensory complex that mediates the endothelial cell response to fluid shear stress. *Nature* 437(7057):426–431.
16. Potter DR, Damiano ER (2008) The hydrodynamically relevant endothelial cell glycocalyx observed in vivo is absent in vitro. *Circ Res* 102(7):770–776.
17. Ho PY, Zhong WB, Ho YS, Lee WS (2006) Terbinafine inhibits endothelial cell migration through suppression of the Rho-mediated pathway. *Mol Cancer Ther* 5(12):3130–3138.
18. Ho PY, Liang YC, Ho YS, Chen CT, Lee WS (2004) Inhibition of human vascular endothelial cells proliferation by terbinafine. *Int J Cancer* 111(1):51–59.
19. Pullamsetti S, et al. (2005) Increased levels and reduced catabolism of asymmetric and symmetric dimethylarginines in pulmonary hypertension. *FASEB J* 19(9):1175–1177.
20. Louden C, et al. (2006) Biomarkers and mechanisms of drug-induced vascular injury in non-rodents. *Toxicol Pathol* 34(1):19–26.
21. Schulz MMP, et al. (2012) Phenotype-based high-content chemical library screening identifies statins as inhibitors of in vivo lymphangiogenesis. *Proc Natl Acad Sci USA* 109(40):E2665–E2674.
22. Kitami T, et al. (2012) A chemical screen probing the relationship between mitochondrial content and cell size. *PLoS One* 7(3):e33755.
23. Qosa H, et al. (2016) High-throughput screening for identification of blood-brain barrier integrity enhancers: A drug repurposing opportunity to rectify vascular amyloid toxicity. *J Alzheimers Dis* 53(4):1499–1516.
24. Kleinstreuer NC, et al. (2014) Phenotypic screening of the ToxCast chemical library to classify toxic and therapeutic mechanisms. *Nat Biotechnol* 32(6):583–591.
25. Ghebes CA, van Lente J, Post JN, Saris DB, Fernandes H (2017) High-throughput screening assay identifies small molecules capable of modulating the BMP-2 and TGF-β1 signaling pathway. *J Biomol Screen* 22(1):40–50.
26. Alves H, Dechering K, Van Blitterswijk C, De Boer J (2011) High-throughput assay for the identification of compounds regulating osteogenic differentiation of human mesenchymal stromal cells. *PLoS One* 6(10):e26678.
27. Laurencin CT, Freeman JW (2005) Ligament tissue engineering: An evolutionary materials science approach. *Biomaterials* 26(36):7530–7536.
28. Blanc A, Pandey NR, Srivastava AK (2004) Distinct roles of Ca2+, calmodulin, and protein kinase C in H2O2-induced activation of ERK1/2, p38 MAPK, and protein kinase B signaling in vascular smooth muscle cells. *Antioxid Redox Signal* 6(2):353–366.
29. Borbiev T, et al. (2003) Role of CaM kinase II and ERK activation in thrombin-induced endothelial cell barrier dysfunction. *Am J Physiol Lung Cell Mol Physiol* 285(1):L43–L54.
30. Lawson ND, Weinstein BM (2002) In vivo imaging of embryonic vascular development using transgenic zebrafish. *Dev Biol* 248(2):307–318.
31. Bayliss PE, et al. (2006) Chemical modulation of receptor signaling inhibits regenerative angiogenesis in adult zebrafish. *Nat Chem Biol* 2(5):265–273.
32. Hirst G, et al. (2006) US Patent 7071199 B1.
33. Arnold LD, et al. (2000) Pyrrolo[2,3-d]pyrimidines containing an extended 5-substituent as potent and selective inhibitors of lck I. *Bioorg Med Chem Lett* 10(19):2167–2170.
34. Endo A, Fukuhara S, Masuda M, Ohmori T, Mochizuki N (2003) Selective inhibition of vascular endothelial growth factor receptor-2 (VEGFR-2) identifies a central role for VEGFR-2 in human aortic endothelial cell responses to VEGF. *J Recept Signal Transduct Res* 23(2-3):239–254.
35. Ferrara N, Gerber H-P, LeCouter J (2003) The biology of VEGF and its receptors. *Nat Med* 9(6):669–676.
36. Tran TC, et al. (2007) Automated, quantitative screening assay for antiangiogenic compounds using transgenic zebrafish. *Cancer Res* 67(23):11386–11392.
37. Kälin RE, Bänziger-Tobler NE, Detmar M, Brändli AW (2009) An in vivo chemical library screen in Xenopus tadpoles reveals novel pathways involved in angiogenesis and lymphangiogenesis. *Blood* 114(5):1110–1122.
38. Patsch C, et al. (2015) Generation of vascular endothelial and smooth muscle cells from human pluripotent stem cells. *Nat Cell Biol* 17(8):994–1003.
39. Orlova VV, et al. (2014) Functionality of endothelial cells and pericytes from human pluripotent stem cells demonstrated in cultured vascular plexus and zebrafish xenografts. *Arterioscler Thromb Vasc Biol* 34(1):177–186.
40. Rufaihah AJ, et al. (2013) Human induced pluripotent stem cell-derived endothelial cells exhibit functional heterogeneity. *Am J Transl Res* 5(1):21–35.
41. White MP, et al. (2013) Limited gene expression variation in human embryonic stem cell and induced pluripotent stem cell-derived endothelial cells. *Stem Cells* 31(1):92–103.
42. Ditadi A, et al. (2015) Human definitive haemogenic endothelium and arterial vascular endothelium represent distinct lineages. *Nat Cell Biol* 17(5):580–591.
43. Therapontos C, Erskine L, Gardner ER, Figg WD, Vargesson N (2009) Thalidomide induces limb defects by preventing angiogenic outgrowth during early limb formation. *Proc Natl Acad Sci USA* 106(21):8573–8578.
44. Kaushal V, Kaushal GP, Melkaveri SN, Mehta P (2004) Thalidomide protects endothelial cells from doxorubicin-induced apoptosis but alters cell morphology. *J Thromb Haemost* 2(2):327–334.
45. Wang C, et al. (2010) Rosuvastatin, identified from a zebrafish chemical genetic screen for antiangiogenic compounds, suppresses the growth of prostate cancer. *Eur Urol* 58(3):418–426.
46. Marchetti F, Romero M, Bonati M, Tognoni G; Collaborative Group on Drug Use in Pregnancy (CGDUP) (1993) Use of psychotropic drugs during pregnancy. A report of the international co-operative drug use in pregnancy (DUP) study. *Eur J Clin Pharmacol* 45(6):495–501.
47. Iqbal MM, et al. (2005) The potential risks of commonly prescribed antipsychotics: during pregnancy and lactation. *Psychiatry (Edgmont)* 2(8):36–44.
48. Vazão H, das Neves RP, Grãos M, Ferreira L (2011) Towards the maturation and characterization of smooth muscle cells derived from human embryonic stem cells. *PLoS One* 6(3):e17771.